



# Novel sulfation effect on low-temperature activity enhancement of CeO<sub>2</sub>-added Sb-V<sub>2</sub>O<sub>5</sub>/TiO<sub>2</sub> catalyst for NH<sub>3</sub>-SCR

Muhammad Salman Maqbool<sup>a,b</sup>, Anil Kumar Pullur<sup>a</sup>, Heon Phil Ha<sup>a,\*</sup>

<sup>a</sup> Center for Materials Architecturing, Korea Institute of Science and Technology, Cheongryang, Seoul 130-650, Republic of Korea

<sup>b</sup> Department of Materials Science, University of Science and Technology, Daejeon 305-350, Republic of Korea

## ARTICLE INFO

### Article history:

Received 6 November 2013

Received in revised form 3 January 2014

Accepted 12 January 2014

Available online 22 January 2014

### Keywords:

CeO<sub>2</sub>/TiO<sub>2</sub>

Cerium(III) sulfate

Beneficial sulfation

NH<sub>3</sub>-SCR

NO<sub>x</sub> conversion

## ABSTRACT

Sulfur dioxide (SO<sub>2</sub>) is considered as a poisoning gas for NH<sub>3</sub>-SCR catalysts under real time conditions. However, it has revealed an obvious beneficial effect on the activity of CeO<sub>2</sub> containing catalysts. Hereby we report the applied research in sulfation effect on low-temperature activity enhancement of CeO<sub>2</sub>-modified, Sb<sub>2</sub>O<sub>3</sub>-V<sub>2</sub>O<sub>5</sub>-TiO<sub>2</sub> catalyst system pretreated with SO<sub>2</sub> under oxidizing conditions at different temperatures for 2 h. We have elucidated the real insights via nature-property relationships of the species formed at various SO<sub>2</sub> pretreatment temperatures (*T* = 300, 400 and 500 °C) with the help of advanced characterization techniques such as X-ray diffraction (XRD), temperature programmed reaction (NH<sub>3</sub>-TPD, NO-TPD and H<sub>2</sub>-TPR), BET surface area, scanning electron microscopy with energy dispersive X-ray spectroscopy (SEM-EDS) and X-ray photoelectron spectroscopy (XPS). Our results indicated that SO<sub>2</sub> pre-treatment at 500 °C led to the maximum favorable sulfation with cerium(III) sulfate as the major surface species.

© 2014 Elsevier B.V. All rights reserved.

## 1. Introduction

The oxides of nitrogen (NO<sub>x</sub>) have been a major source of air pollution. The major sources of NO<sub>x</sub> are the combustion of fossil fuels, particularly petroleum and its products in vehicle engines as well as coke in thermal power plants [1–3]. NO<sub>x</sub> (*x* = 1, 2) emissions can cause adverse effects to the environment and human health through increasing ground level ozone by reacting with volatile organic compounds (VOC) and particulate matter. The reduction of NO<sub>x</sub> emissions by NH<sub>3</sub>-SCR (selective catalytic reduction) is one of the most efficient technologies used for eliminating NO<sub>x</sub> from stationary power plants and diesel engines exhaust.

The well-known commercial catalysts such as V<sub>2</sub>O<sub>5</sub>-WO<sub>3</sub> (or MoO<sub>3</sub>)/TiO<sub>2</sub> have been widely used for decades [4,5]. The addition of WO<sub>3</sub> and/or MoO<sub>3</sub> to V<sub>2</sub>O<sub>5</sub>/TiO<sub>2</sub> can increase the activity and stability for NH<sub>3</sub>-SCR in the temperature window of 290–420 °C, reduce ammonia oxidation, and greatly increase the poison resistance to alkali and arsenious oxides. Although the vanadia based catalysts have been commercialized for the SCR technology, still there is room for improvement in low-temperature activity under abundant SO<sub>2</sub> conditions. The main problems related to NH<sub>3</sub>-SCR catalysts based on vanadia include high activity for SO<sub>2</sub> oxidation to SO<sub>3</sub>, formation of N<sub>2</sub>O at high temperatures, and toxicity of vanadia. The formed SO<sub>3</sub> can cause additional problems because SO<sub>3</sub>

combines with H<sub>2</sub>O, and results in NH<sub>3</sub>-slip to form ammonium sulfates and H<sub>2</sub>SO<sub>4</sub> that lead to pore plugging of the catalysts and corrosion of the equipment at low temperatures (<250 °C) [6–8].

In the past decades, great efforts have been devoted to the improvement of low-temperature sulfur-resistance of V<sub>2</sub>O<sub>5</sub> based catalysts for NH<sub>3</sub>-SCR [6,9–11]. Such studies reveal that the SO<sub>2</sub> has complicated effect on SCR activity, however deactivating the catalysts at temperatures below 300 °C. Previous investigations by Orsenigo et al. [7] compared effects of sulfation on NO<sub>x</sub> reduction and SO<sub>2</sub> oxidation activities, suggesting that the sulfation occurs first on vanadia sites and later on TiO<sub>2</sub> and tungsten sites. The sulfur species formed on the catalyst surface either enhance or reduce catalyst activity depending on their nature and properties [12–14]. It is also reported that the surface sulfate species formed after sulfation strengthened the active Brønsted acid sites which may increase and stabilize catalyst activity [15].

Recently, ceria (CeO<sub>2</sub>) has received considerable attention for NH<sub>3</sub>-SCR because of its high oxidation and reduction abilities which promote NO oxidation at low temperatures. Ceria-mixed oxide catalysts, such as Ce-Cu-Ti oxides [16], Mn-Ce/TiO<sub>2</sub> [17,18], CeO<sub>2</sub>/TiO<sub>2</sub> [19], Ce<sub>x</sub>Ti<sub>1-x</sub>O<sub>2</sub> [20], CeO<sub>2</sub>-WO<sub>3</sub>/TiO<sub>2</sub> [21] and CeO<sub>2</sub>-WO<sub>3</sub> [22] have shown excellent NH<sub>3</sub>-SCR activity and N<sub>2</sub> selectivity, but poor sulfur tolerance. Chang et al. reported that MnO<sub>x</sub>-CeO<sub>2</sub> mixed oxide catalyst showed high resistance to SO<sub>2</sub> with the addition of Sn [23]. This positive effect is most probably due to the formation of more cerium(III) sulfates [24]. However, at temperatures below 300 °C, it still remains a big challenge to develop sulfur-tolerant catalysts for NH<sub>3</sub>-SCR.

\* Corresponding author. Tel.: +8229585461; fax: +8229585599.

E-mail address: [heonphil@kist.re.kr](mailto:heonphil@kist.re.kr) (H.P. Ha).

In our latest studies for  $\text{NH}_3$ -SCR of  $\text{NO}_x$ , we have reported ceria-added  $\text{Sb-V}_2\text{O}_5/\text{TiO}_2$  catalyst, which showed high sulfur tolerance at  $240^\circ\text{C}$  [25,26]. The aim of the present work is to investigate the real nature of beneficial sulfate and its role in low-temperature activity enhancement of ceria-added  $\text{Sb-V}_2\text{O}_5/\text{TiO}_2$  catalyst. The as-prepared and sulfated catalysts were characterized by X-ray diffraction (XRD), Temperature programmed desorption/reduction (TPD/R), Brunner–Emmett–Teller surface area (BET-SA), X-ray photoelectron spectroscopy (XPS) and scanning electron microscopy (SEM). The current study is considered to be of great importance with regards to its application under severe  $\text{SO}_2$  and  $\text{H}_2\text{O}$  conditions.

## 2. Experimental

### 2.1. Catalyst preparation

The  $\text{CeO}_2$  modified,  $\text{Sb-V}_2\text{O}_5/\text{TiO}_2$  catalysts were prepared by incipient wetness co-impregnation and deposition–precipitation methods, as discussed in our previous report [25]. The synthesized sample after calcination was denoted as “as-prep.” For sulfated catalysts, the as-prepared samples were treated with  $\text{SO}_2$  (500 ppm) and  $\text{O}_2$  (3%) with balance  $\text{N}_2$  for 2 h at various (300, 400 and  $500^\circ\text{C}$ ) temperatures. The samples were then labeled as S300, S400 and S500, respectively.

### 2.2. Physico-chemical characterization

The BET (Brunauer–Emmett–Teller) surface area was measured from the  $\text{N}_2$  adsorption and desorption isotherms at  $-196^\circ\text{C}$  using the ASAP-2010 (Micromeritics) analyzer. The catalysts were analyzed by powder X-ray diffraction (Bruker) and the spectra were recorded using Ni-filtered  $\text{Cu K}\alpha$  radiation operated at 40 kV and 40 mA. Due to unknown level of homogeneity of the sulfate species formed in pretreated catalysts, the samples were rotated at a rotation speed of 15 rpm during analysis.  $\text{NH}_3$  and  $\text{NO}$  TPD experiments were carried out using the AutoChem II-2920 (Micromeritics) chemisorptions analyzer. For each experiment, 100 mg of catalyst was placed in a U-shaped quartz cell and preconditioned at  $120^\circ\text{C}$  in He gas at a flow rate of  $50\text{ mL min}^{-1}$ . Accordingly, 1%  $\text{NH}_3$  and 1%  $\text{NO}$  under He balance were used as adsorption media ( $50\text{ mL min}^{-1}$  flow) at  $50^\circ\text{C}$  for 60 min. Furthermore, the samples were heated to  $100^\circ\text{C}$ , purged with He gas to remove the physically adsorbed gases, and cooled down to the starting point of  $50^\circ\text{C}$ . Afterwards, the TPD run was conducted from 50 to  $550^\circ\text{C}$  at a heating rate of  $10^\circ\text{C min}^{-1}$ . Simultaneously, TPD–mass spectra were analyzed by HPR-20 QIC (Quartz Inert Capillary) (HIDEN analytical) real time gas analyzer (RGA) for multiple species of molecular weight up to 300 amu. The quantity of  $\text{NH}_3$  ( $\text{NH}_3$ -TPD) was calculated by measuring the average area of 5 consecutive 1 cc volume pulse injections (similar areas) of 5%  $\text{NH}_3/\text{He}$  gas.  $\text{H}_2$ -TPR experiments were carried out by heating the catalysts (each 100 mg) at a linear heating rate of  $10^\circ\text{C min}^{-1}$  between 50 and  $900^\circ\text{C}$  with 10%  $\text{H}_2/\text{Ar}$  at a constant flow rate of  $50\text{ mL min}^{-1}$ . XPS studies were carried out by using PHI 5800 ESCA system, employing a non-monochromatic  $\text{Al K}\alpha$  (1486.6 eV) source. The binding energies were referenced to the C 1s line at 284.6 eV from adventitious carbon. Scanning electron microscopy (SEM) images were taken by Hitachi S-4200 FE-SEM equipped with EDS (energy dispersive X-ray spectroscopy) at an acceleration voltage of 15 kV.

### 2.3. Activity measurements

The SCR of  $\text{NO}_x$  ( $\text{NO} + \text{NO}_2$ ) over the synthesized catalytic materials was evaluated by using ammonia as a reductant. The conversion of  $\text{NO}_x$  was determined over a down flow fixed-bed reactor system.

**Table 1**

Physical properties of as-prepared and sulfate samples at different temperatures.

Sample name	BET surface area ( $\text{m}^2/\text{g}$ )	Pore diameter (nm)	Pore volume ( $\text{cm}^3/\text{g}$ )
As-prep.	54.4	20.0	0.28
S300	57.8	18.1	0.27
S400	62.0	17.4	0.29
S500	58.7	16.3	0.26

The quartz reactor (1 cm o.d. and 50 cm length) was placed vertically in a tubular furnace connected to a temperature controller indicator. To minimize the mass transfer limitations, the catalyst was sieved with 40–50 mesh size and then charged into the quartz reactor using quartz wool. Prior to each experiment, about 0.5 mL catalyst was pre-treated by a mixture of 3%  $\text{O}_2$  and  $\text{N}_2$  flowing at  $500^\circ\text{C}$  for 1 h. A reaction stream consisting of 800 ppm  $\text{NO}_x$ , 800 ppm  $\text{NH}_3$ , 3 vol.%  $\text{O}_2$ , 6 vol.%  $\text{H}_2\text{O}$ , 500 ppm  $\text{SO}_2$  and  $\text{N}_2$  balance was fed into the reactor system through mass flow controllers with a total flow rate of  $500\text{ mL min}^{-1}$  and at a space velocity of  $60,000\text{ h}^{-1}$ . Water vapor was produced by passing  $\text{N}_2$  gas through a heated glass wash bottle containing de-ionized water. Catalytic activity measurements were performed in a top-down pattern over a low temperature range ( $350$ – $175^\circ\text{C}$ ). Additionally, the stability tests for as-prepared and sulfated catalysts were carried out at  $225^\circ\text{C}$  for 5 h. For each stability test, in case of sulfation pretreatment involved, the temperature was decreased directly from the sulfation temperature (in the presence of 3%  $\text{O}_2$  and  $\text{N}_2$  balance) to  $225^\circ\text{C}$ . The effluent from the reactor was analyzed by an online NDIR Fuji  $\text{NO}$  and  $\text{SO}_2$  analyzer.  $\text{NO}_2$  amount was determined by converting  $\text{NO}_2$  into  $\text{NO}$  with Gas converter series CG-2M analyzer. The percentage conversion of  $\text{NO}_x$  was calculated by using the formula given below.

$$\text{NO}_x \text{ conversion} = \left( \frac{[\text{NO}_x]_{\text{in}} - [\text{NO}_x]_{\text{out}}}{[\text{NO}_x]_{\text{in}}} \right) \times 100 \quad (1)$$

## 3. Results and discussion

### 3.1. Catalyst characterization

#### 3.1.1. BET surface area

Physical properties of a catalyst such as, surface area, pore diameter and pore volume are very important to determine the adsorption–desorption phenomena of gases onto its surface. Table 1 compares these physical measures for fresh and sulfated catalysts at different temperatures. Interestingly, all the sulfated catalysts showed an increment in the BET surface area after sulfation pretreatment. This gives a clue about the formed sulfates to be amorphous in nature. Moreover, pore diameter of the catalysts was reduced after sulfation, especially in case of the sample treated at  $500^\circ\text{C}$ . Since the amount of  $\text{SO}_2$  used during pretreatment also increased with increasing temperature, these sulfates seem to enter the pores of the catalysts, thereby decreasing both the pore diameters and pore volumes of the sulfated catalysts.

#### 3.1.2. X-ray diffraction (XRD) studies

Fig. 1 illustrates the XRD patterns for the fresh and sulfated catalysts along with the possible cerium sulfates. The as-prepared catalyst exhibited characteristic  $\text{CeO}_2$  [PDF-ICDD 81-0792] and  $\text{TiO}_2$ -anatase [PDF-ICDD 86-1157] peaks. The peaks corresponding to  $\text{Sb}_2\text{O}_3$  and  $\text{V}_2\text{O}_5$ , could not be detected possibly because of their nominal addition and well-dispersion of the oxides. Furthermore, no  $\text{CeO}_2$  peak could be observed in any of the sulfated catalysts, which could suggest preferential sulfation of ceria lessening its crystallinity [24]. It is also important to note that none

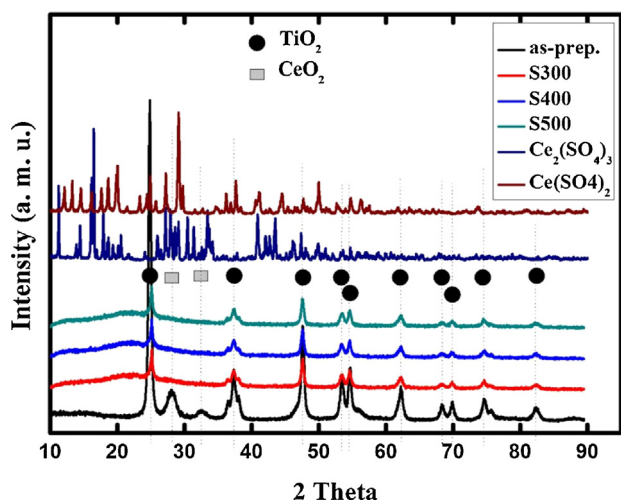


**Fig. 1.** XRD patterns of the catalysts, as-prepared and sulfated at different temperatures along with commercial  $\text{Ce}_2(\text{SO}_4)_3$  and  $\text{Ce}(\text{SO}_4)_2$ .

of the possible cerium sulfates could be observed in the sulfated samples. This implies that either the formed sulfates were too low in the quantity to be detected by XRD, or amorphous in nature.

### 3.1.3. SEM and EDS analyses

In order to determine their morphology, all the fresh and sulfated samples were characterized by FE-SEM (Field emission scanning electron microscopy). The resultant micrographs of the studied catalysts have been demonstrated in Fig. 2. However, the images could not present any obvious difference among the fresh and sulfated catalysts at various temperatures. Therefore energy dispersive spectroscopy (EDS) of the samples was carried out in order to detect the amount of sulfur in sulfated catalysts, and the resultant peak intensities have been presented in Fig. 3. In case of sulfated catalysts, an additional peak of sulfur was observed.

Moreover, similar to our  $\text{SO}_2$  usage data during sulfation pretreatment, more sulfur amount was detected in S500 sample (not shown here), which confirms the formation of relatively more sulfate species than in the samples sulfated at low temperatures (S300 and S400).

### 3.2. Activity measurement

Effect of sulfation pretreatment in the oxidizing environment on low-temperature activity of the catalyst was observed in terms of  $\text{NO}_x$  conversion over a temperature range of 350–175 °C (Fig. 4a). All the samples showed 100%  $\text{NO}_x$  conversion (except 97% for S300) at temperatures  $\geq 250$  °C due to active redox species such as  $\text{V}_2\text{O}_5$  and  $\text{CeO}_2$  [11,27]. However below 250 °C, the activity declined most probably due to the formation of both low-temperature sulfate species as well as ammonium bisulfate (ABS). Among all the samples, the highest activity in low-temperature range was shown by S500 catalyst, which suggests that the sulfates formed at 500 °C are the most favorable for  $\text{NH}_3$ -SCR of  $\text{NO}_x$ . Contrastingly, the activity measurements at low temperatures ( $\leq 250$  °C) for other three samples could not illustrate a clear difference, possibly due to lower resistance against  $\text{SO}_2$ -poisoning. However  $\text{SO}_2$  usage data, (shown in Fig. 4b), suggests that the tendency of sulfate formation is lower onto the pre-sulfated catalysts at higher temperatures ( $\geq 250$  °C). This might be due to repulsive interaction between  $\text{SO}_2$  and the pre-formed sulfates. The as-prepared catalyst consumed more amount of  $\text{SO}_2$  during the course of reaction. This could be due to consumption of  $\text{SO}_2$  by catalyst itself for cerium sulfate formation, as well as to form the ammonium sulfates. However, the formed initial sulfate species on the as-prepared catalysts seemed undamaging for the  $\text{NH}_3$ -SCR. So, the as-prepared catalyst showed slightly higher activity than that of S300 catalyst at low temperatures. While the sulfate species on as-prepared catalyst were formed at a temperature far less than 500 °C. As a consequence, the as-prepared catalyst showed lower activity than S500, which suggests that the sulfates formed at 500 °C are the most favorable for  $\text{NH}_3$ -SCR.

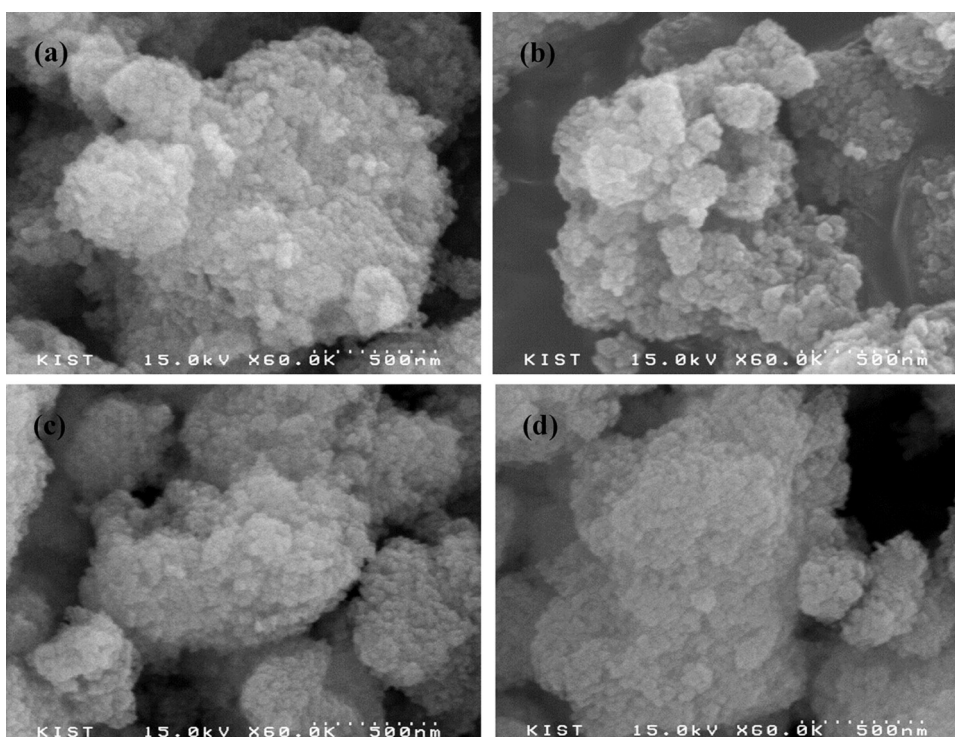


**Fig. 2.** SEM images of the catalysts, as-prepared and sulfated at different temperatures: as-prep., (b) S300, (c) S400, and (d) S500.



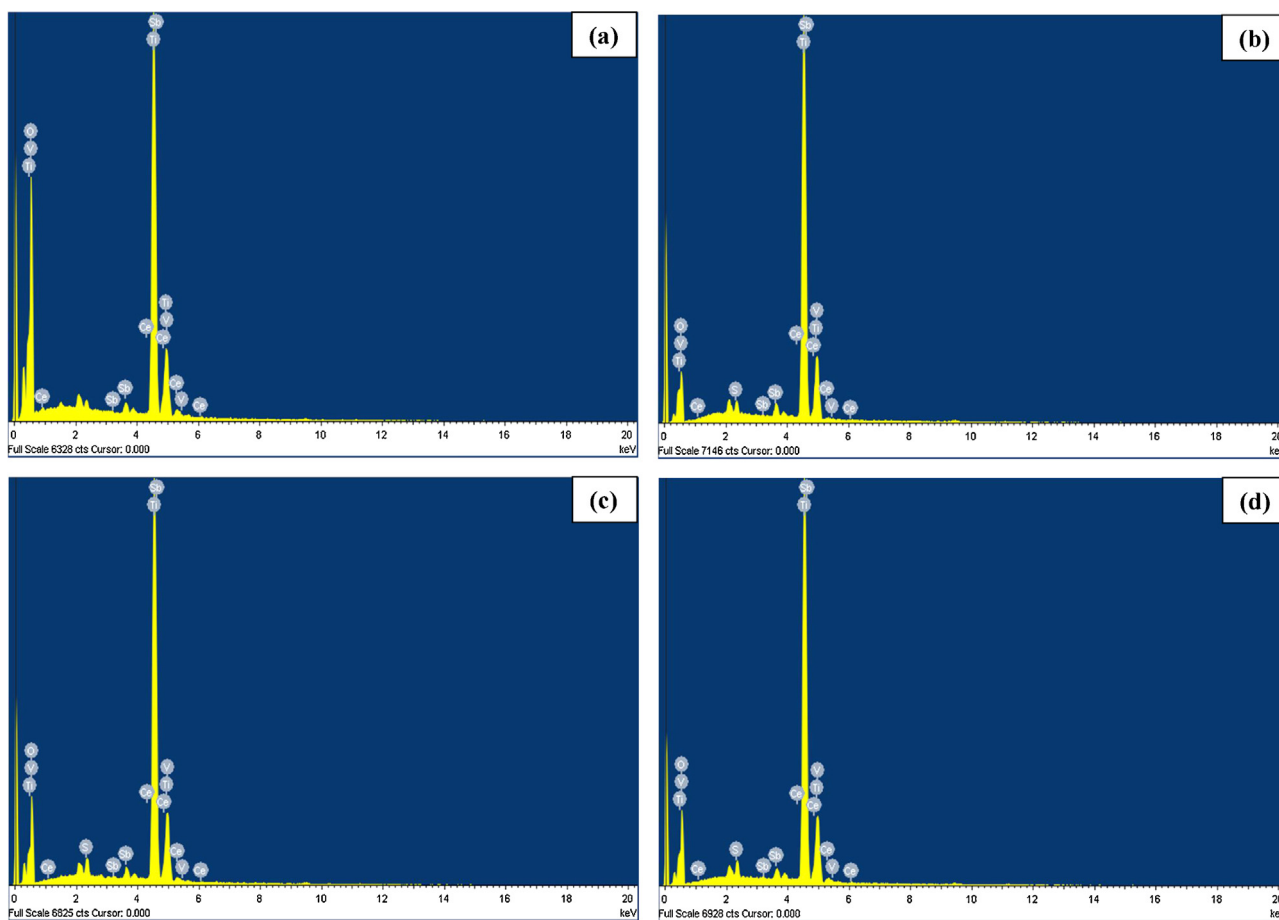


Fig. 3. Elemental peak intensities from energy dispersive spectroscopy (EDS): as-prep., (b) S300, (c) S400, and (d) S500.

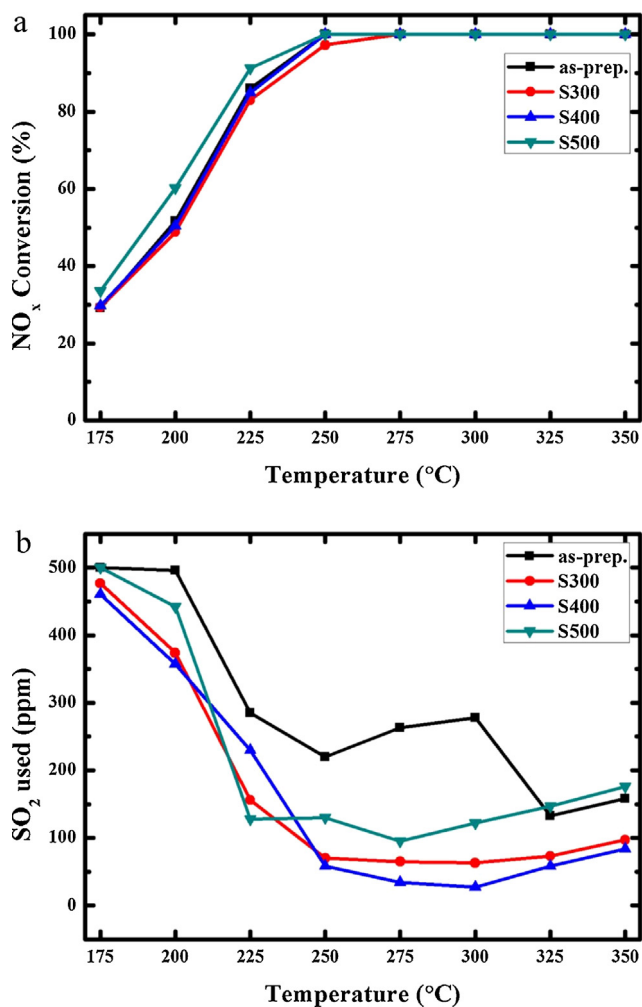
In order to have a closer look on effect of sulfation pretreatment at low-temperature activity, all the catalysts were subjected to stability tests at 225 °C for 5 h. The as-prepared catalyst (without any sulfation treatment), showed 83% conversion which underwent an ordinary change in its activity ( $\approx 80\%$  conversion) after the total runtime of 5 h. The sample pretreated at 300 °C for 2 h (S300) started with a slightly higher activity ( $\approx 85\%$  conversion) however suffered from deactivation after 5 h ( $\approx 75\%$  conversion). This deactivation might be due to less favorable, low temperature sulfate species formed during sulfation pretreatment at 300 °C. Yang et al. have reported similar results for  $\text{CeO}_2$  catalyst, where  $\text{SO}_2 + \text{O}_2$  pretreated samples at 300 °C for 8 h showed poor activity as compared to that of a fresh sample at low temperatures under  $\text{SO}_2$  conditions [27]. The catalyst treated at next higher temperature i.e., 400 °C (S400) showed an improved catalytic activity initially ( $\approx 88\%$  conversion) when compared to as-prepared and S300 catalysts. However, its activity was also declined, and reached a value closer to that of as-prepared sample after 5 h run (81%). The activity shown by S500 C was the highest and most sustainable among all. It showed a  $\text{NO}_x$  conversion of  $\approx 94\%$ , and could retain its activity around 90% after 5 h. The above results have suggested a positive impact of sulfation pretreatment under oxidizing conditions on the Ce-modified  $\text{Sb-V}_2\text{O}_5/\text{TiO}_2$  catalyst. All the pretreated samples, when compared to as-prepared catalysts, have shown an improved activity at the start. However, the pretreatment temperature has been proved to be a critical measure for long-term stability of the catalyst at low temperature.

Fig. 5b represents the comparison for amount of  $\text{SO}_2$  used (ppm) by each catalyst during and after sulfation pretreatment. It can be clearly seen that a lot of  $\text{SO}_2$  was used during sulfation of the

catalyst at highest temperature (500 °C) throughout pretreatment duration. This  $\text{SO}_2$  used is supposed to form beneficial cerium sulfate species most probably on the surface of the catalyst, as discussed later. However, as the pretreatment temperature was decreased, only a small amount of  $\text{SO}_2$  was consumed for the purpose. This suggests that the sulfation temperature is an important factor for the formation of surface sulfate species on the catalyst. The sulfation under given oxidizing environment seems to be kinetically favorable at higher temperatures.

In order to confirm that the origin of beneficial sulfation was from  $\text{CeO}_2$  component of the catalyst system, a  $\text{Sb-V}_2\text{O}_5/\text{TiO}_2$  catalyst (without  $\text{CeO}_2$  addition) [28] was evaluated for its catalytic performance with and without sulfation treatment. The resultant activity graphs are shown in Fig. 6a. It can be clearly seen that, despite similar composition, no activity improvement could be observed for catalyst without  $\text{CeO}_2$ . Oppositely, the activity was decreased over time after sulfation treatment, most probably due to formation of ammonium bisulfate (ABS) species at such a lower temperature [6,29]. From  $\text{SO}_2$  usage data presented in Fig. 6b, it can be observed that a lot of  $\text{SO}_2$  was used with the passage of time, especially for the sulfated sample which seemed to be poisoned by sulfation.

The effect of sulfation on  $\text{NH}_3$ -SCR activity of the catalysts has been a matter of debate for a decade or two. Based on our literature review, the promotional effect of  $\text{SO}_2$  in the presence of  $\text{H}_2\text{O}$  on  $\text{V}_2\text{O}_5/\text{TiO}_2$  catalysts was first reported by Amiridis et al. [11]. They found that during the SCR reaction of NO by  $\text{NH}_3$ , the turnover frequency at low surface vanadia coverage was enhanced with the presence of  $\text{SO}_2$  in the reaction gas stream, without any maximum at vanadia loadings exceeding half a monolayer. As a conclusion,



**Fig. 4.** Effect of sulfation pretreatment temperature on the activity at low temperatures: (a) NO<sub>x</sub> conversion and (b) amount of SO<sub>2</sub> used (reaction conditions: [NO<sub>x</sub>] = [NH<sub>3</sub>] = 800 ppm, [O<sub>2</sub>] = 3 vol.%, H<sub>2</sub>O = 6 vol.%, SO<sub>2</sub> = 500 ppm, N<sub>2</sub> balance, GHSV = 60,000 h<sup>-1</sup>).

they ascribed the beneficial effect of SO<sub>2</sub> to strong Brønsted acidic sites by the reaction between H<sub>2</sub>O and SO<sub>2</sub>, existing in the form of surface sulfates. From our results presented in Fig. 5a, it could be clearly seen that the sulfation at low temperatures (300 and 400 °C) could be detrimental for the catalyst activity. Despite the formation of quite few cerium sulfates, both the catalysts (S300 and S400) showed declined activities at low temperature as compared to that of S500 catalyst. While it is important to note that the activity of as-prepared sample remained almost unchanged throughout the activity run of 5 h. Since the as-prepared catalyst used up around 150–170 ppm SO<sub>2</sub> in the first 4 h of run, it can be concluded that the initial sulfation of the catalyst resulted preferably in the formation of Ce-sulfates. On the contrary, the activity curve of S300 catalyst surprisingly followed a steep slope after about 2 h of activity measurement. This suggests another view point that the sulfates formed at low temperatures (<500 °C) might differ in nature from those formed at high temperatures. Therefore, in order to differentiate between them, the sulfate species formed at 300 and 500 °C will be termed from now onwards as ‘low-temperature sulfates’ and ‘high-temperature sulfates’, respectively. Contrastingly, the sulfates formed at 400 °C were thought to have mixed nature of low- as well as high-temperature sulfates, as discussed in details later on.

Xie et al. [30] reported the promotional effect of SO<sub>2</sub> on SCR activity of CuO/Al<sub>2</sub>O<sub>3</sub> catalyst sorbent due to the formation

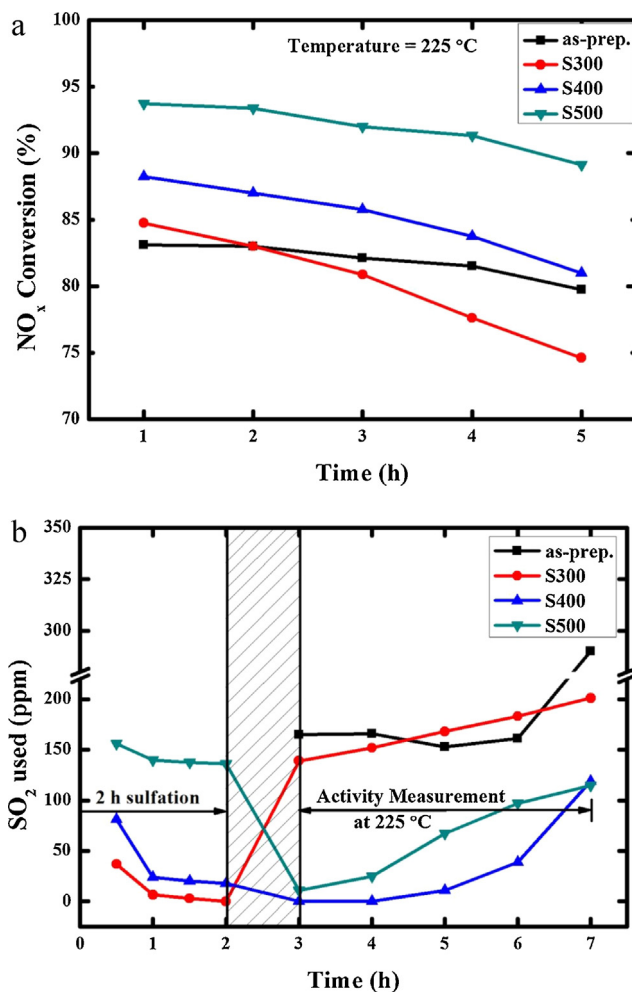


**Fig. 5.** Effect of sulfation pretreatment temperature on stability of the catalysts at 225 °C: (a) NO<sub>x</sub> conversion and (b) amount of SO<sub>2</sub> used (reaction conditions: same as given in Fig. 4).

of sulfate species. However, they could find out that the sulfates formed at temperatures below 300 °C were not active enough for NH<sub>3</sub>-SCR of NO. We have also noticed a similar trend for our catalyst, where the sample pretreated at 300 °C underwent deactivation badly. The beneficial effect of sulfation over CeO<sub>2</sub> for NH<sub>3</sub>-SCR of NO<sub>x</sub> over a wide temperature range (275–525 °C) was reported first by Gu et al. [24]. Based on our results, it is obvious that the temperature of sulfation should be higher than 400 °C in order to promote low temperature activity by the formation of beneficial surface cerium sulfates.

### 3.3. Supportive characterization

#### 3.3.1. NH<sub>3</sub>-TPD

The amount and strength of acidic sites present on the surface of a catalyst can be determined through adsorption/desorption studies of a basic gas i.e., NH<sub>3</sub>. The samples were heated from 50 to 550 °C in order to find out the NH<sub>3</sub>-desorption behavior for the catalysts, and the curves obtained are depicted in Fig. 7. All the catalysts showed two peaks: first one in the range around 100–300 °C, and the second one in the range around 300–450 °C. The as-prepared (fresh) catalyst showed lowest amount of acidic sites as compared to sulfated catalysts. Yang et al. [27] and Gao et al. [31] also reported that the number of acidic sites is increased upon sulfation. The amount and strength of acidic sites on S300 sample were much higher than those found in S400 and S500.

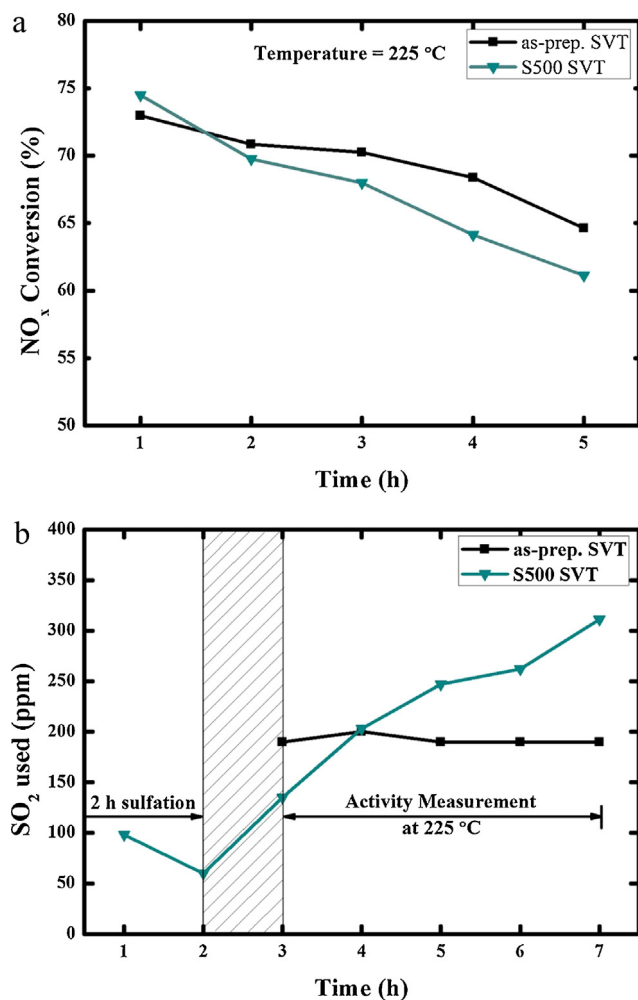


**Fig. 6.** Effect of sulfation pretreatment on stability of the catalyst Sb-V<sub>2</sub>O<sub>5</sub>/TiO<sub>2</sub> (without CeO<sub>2</sub>) at 225 °C: (a) NO<sub>x</sub> conversion and (b) amount of SO<sub>2</sub> used (reaction conditions: same as given in Fig. 4).

This strong and excessive adsorption of NH<sub>3</sub> could inhibit the catalyst performance at lower temperatures [32]. Nova et al. could propose a number of reasons for this NH<sub>3</sub>-inhibition effect. Firstly the excess ammonia might adsorb onto the pre-adsorbed NH<sub>3</sub>, without any activation and interaction with gaseous NO. Secondly

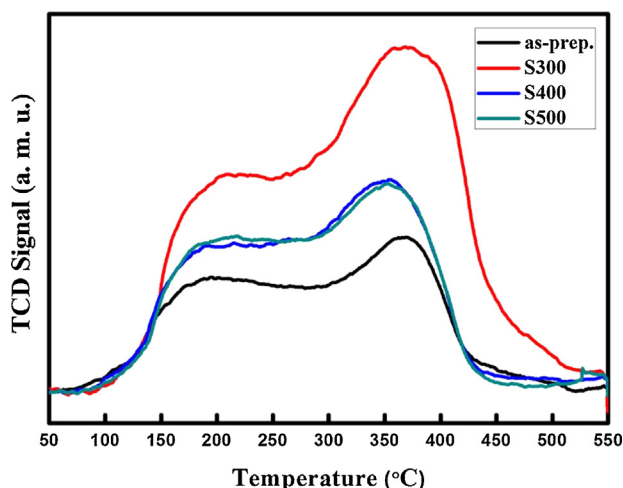


**Fig. 7.** NH<sub>3</sub>-TPD profiles of the catalysts, as-prepared and sulfated at different temperatures.

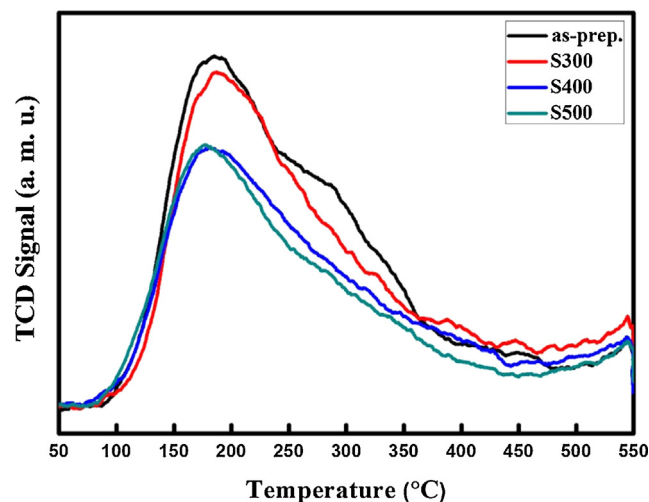


**Fig. 8.** NO-TPD curves for the catalysts, as-prepared and sulfated at different temperatures.

beneficial, competitive NO adsorption and activation, reported for active oxide-based systems for NH<sub>3</sub>-SCR [4], could be prohibited by excess NH<sub>3</sub> adsorption. Thirdly quite closer to our catalyst system, NH<sub>3</sub> adsorbed onto an acidic site in the vicinity of redox specie could exacerbate its function either by blocking it or through interaction between their electrons. Both S400 and S500 could barely show a difference in strength of their acidic sites. By having a closer look on mass spectra (Fig. S1a and S1b), S300 sample showed the highest NH<sub>3</sub> desorption, followed by S400 and S500 respectively. Interestingly, S300 catalyst also showed highest NO<sub>x</sub> formation by NH<sub>3</sub> oxidation. Based on our activity results, the sulfates formed on S300 catalyst seemed to be inactive for NH<sub>3</sub> activation to reduce NO. Comparatively, S400 catalyst showed intermediate activity between those of S300 and S500 catalysts. Therefore, it suggests that the nature of sulfates species formed on S400 catalyst is a mixture of those present in S300 and S500 samples. The sulfate species formed on S500 could be the most active species for NH<sub>3</sub> activation, showing improved and sustainable NO<sub>x</sub> conversion.

### 3.3.2. NO-TPD

In order to compare the NO adsorption behavior of as-prepared and the sulfated catalysts, NO-TPD was carried out; and the resultant patterns have been presented in Fig. 8. Only as-prepared catalyst could show two peaks: first, large one at 187 °C and second, small neck at 290 °C. The first peak could be assigned to low-strength basic sites which released physisorbed NO upon heating. The second peak at higher temperature might show the chemisorbed NO, released from the fresh CeO<sub>2</sub> sites (based on its acid-base properties). Contrastingly, all the sulfated samples showed only single desorption peak at low temperatures with comparatively smaller area. This is an indication of increased acidity of the catalysts after being sulfated. Moreover, the amounts of NO desorbed were variables among the three samples sulfated at different temperatures. This might support the view point that the sulfate species formed at different pretreatment temperatures were dissimilar in their nature. As compared to fresh sample, S300 showed quite low NO adsorption [27]. However, highest NO desorption was observed on S300 sample among the catalysts sulfated at different temperatures (Fig. S2). Both the S400 and S500 catalyst samples showed more or less same NO desorption peak, whereas slightly higher amount of NO desorption was detected for S500 sample than that on S400 at low temperatures (150–275 °C). This could be another reason for higher activity shown by S500 sample than the other sulfated samples.

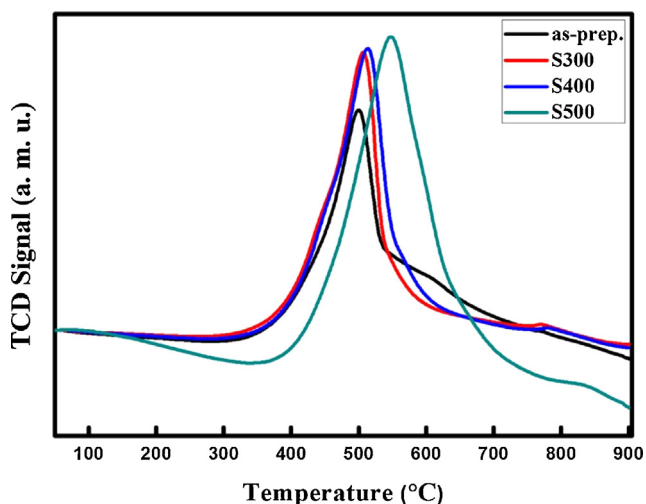


Fig. 9.  $H_2$ -TPR profiles of the catalysts, as-prepared and sulfated at different temperatures.

### 3.3.3. $H_2$ -TPR

The availability and amount of reducible species present on fresh and sulfated catalysts were determined through  $H_2$ -TPR. The curves obtained from as-prep., S300, S400 and S500 are illustrated in Fig. 9. All the samples showed two distinct peaks, a large area peak in the range of 300 to 700 °C and a small area peak at higher temperatures around 700 to 900 °C. The low-temperature peaks could arise from reduction of the surface species such as  $Sb^{5+}$ ,  $V^{5+}$ ,  $Ce^{4+}$  and the sulfates [25]. The as-prepared catalyst showed comparatively smaller reduction peak, and slightly at lower  $T_{max}$  (maximum peak reduction temperature) than those of the sulfated samples. This mainly included reduction of  $Sb^{5+}$  to  $Sb^{3+}$ ,  $V^{5+}$  to  $V^{3+}$ , and  $Ce^{4+}$  to  $Ce^{3+}$ . Their respective mass spectra data for reduction of oxide species has been presented in Fig. 10. On the other hand, the additional peak area of the sulfated catalysts could arise mainly from the sulfates after  $SO_2$  pretreatment. The  $H_2O$ ,  $SO_2$  and  $O_2$  mass spectra were detected (Fig. 10a, b and c respectively), which can be assigned to reduction of the oxide species to  $H_2O$ , and the decomposition of sulfate species essentially to  $SO_2$  and  $O_2$ . Interestingly, the  $T_{max}$  of sulfated catalysts were different from one another, and shifted towards right with increase of sulfation temperature. Again, this gives an indication that the sulfates formed at various temperatures are dissimilar in their nature. The samples pretreated at 300 and 400 °C showed a closer  $T_{max}$  (around 512 °C), whereas sample pretreated at 500 °C showed a peak maximum at around 551 °C. This difference in peak maxima confirms that the sulfates formed at higher temperatures are different in nature compared to the low-temperature sulfates. According to the literature data, the sulfate species could be reduced at high temperatures [33,34]. Similarly, the sulfated samples showed broad peaks with more consumption of  $H_2$  as compared to as-prepared catalyst. During sulfation process, the sulfated species formed on the ceria are more predominated than the other vanadia, antimony and titania species. It could be due to the higher affinity of ceria with  $SO_2$ . In addition, the beneficial sulfation effect was observed in Ce-added catalysts only, as reported previously [25]. In our results we found that the reduction temperatures of S500 samples are higher than those of S400 and S300 catalysts. Simultaneously, the  $H_2O$ ,  $SO_2$  and  $O_2$  mass spectra (Fig. 10a, b and c) confirm their evolution at higher temperatures on S500 catalyst as compared to S400 and S300. Comparing with their decomposition temperatures provided in literature [35,36], these results suggest that the formed sulfate species on S500 and S300 catalysts correspond to Ce(III) sulfate and Ce(IV) sulfates, respectively. On the other hand, the sulfate species

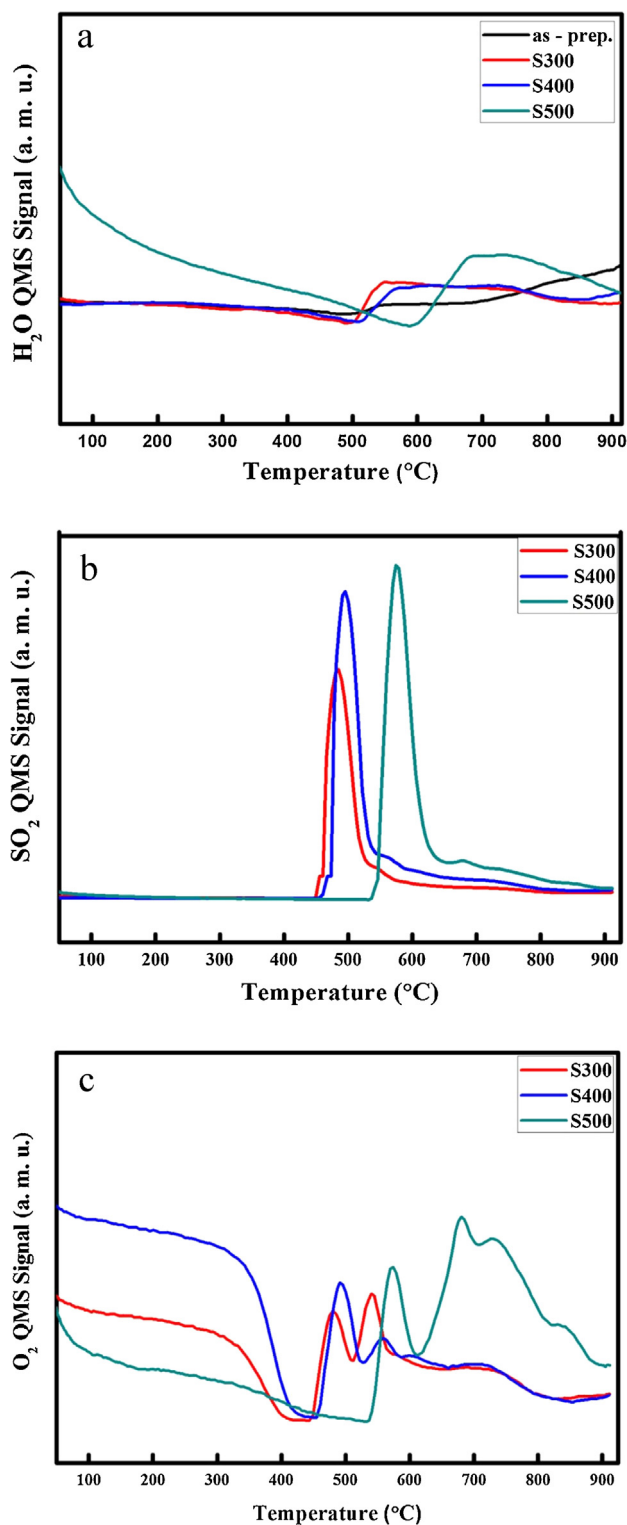


Fig. 10. Mass spectra of  $H_2$ -TPR for the catalysts, as-prepared and sulfated at different temperatures: (a)  $H_2O$ , (b)  $SO_2$ , and (c)  $O_2$  signals.

formed on S400 catalysts contain mixture of Ce(IV) and Ce(III) sulfate species. Moreover, the reduction peak area of S500 catalyst was larger than those pretreated at lower temperatures, indicating higher amounts of sulfates species present on its surface. This observation is in line with  $SO_2$  usage data during  $SO_2$  pretreatment. The second small peak observed at temperatures higher than 700 °C for all the catalysts could be assigned to the reduction of bulk ceria



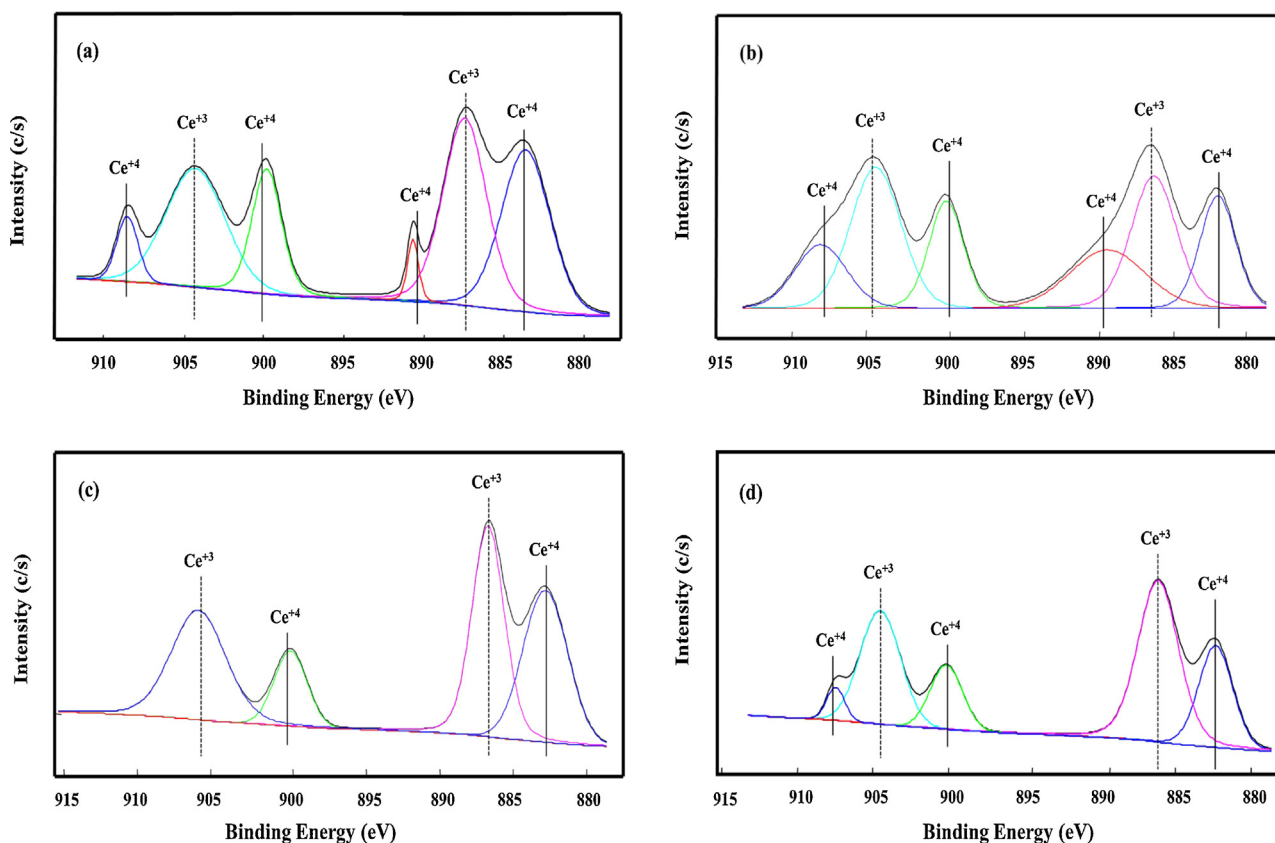


Fig. 11. XPS spectra of Ce 3d for the catalysts, as-prepared and sulfated at different temperatures: (a) as-prep., (b) S300, (c) S400, and (d) S500.

which was readily available after reduction of the surface sulfate species.

### 3.3.4. XPS studies

The XPS studies were carried out on all the fresh and sulfated catalysts in order to know surface atomic concentrations, and ratios of their different oxidation states. The curves from XPS are depicted in Figs. 11–13, whereas surface elemental compositions have been presented in Table 2. Fig. 11 shows the Ce peak fit for as-prepared, S300, S400 and S500 catalyst samples. The as-prepared catalyst consisted of a balanced  $\text{Ce}^{3+}$  and  $\text{Ce}^{4+}$  compositions that provided with reasonably higher activity at temperature as low as  $225^\circ\text{C}$  [37]. However when the sulfation was carried out at  $300^\circ\text{C}$ , the amount of  $\text{Ce}^{4+}$  species was increased compared to the as-prepared sample. This increase in  $\text{Ce}^{4+}$  species might be due to the formation of  $\text{Ce(IV)}$  sulfate species on its surface. On the other hand, both S400 and S500 samples showed an increase in  $\text{Ce}^{3+}$  content, with S500 having higher content. This increased  $\text{Ce}^{3+}$  concentrations in these samples after sulfation can be related to the formation of  $\text{Ce(III)}$  sulfate species. Therefore, it can be concluded that the cerium sulfate species formed at different pretreatment temperatures are unlike in their nature. Moreover, the amounts of  $\text{Ce(III)}$  species are more abundant on the surface of S500 catalyst. Based on our activity results, it could be inferred that  $\text{Ce(III)}$  sulfate species are highly active for  $\text{NH}_3$ -SCR of  $\text{NO}_x$ , and are formed in abundance at high temperature ( $500^\circ\text{C}$ ) pretreated catalysts. These  $\text{Ce(III)}$  species (in the form of sulfate) could favor  $\text{NH}_3$  adsorption and activation, whereas the rest of  $\text{Ce}^{4+}$  species (in the form  $\text{CeO}_2$ ) could adsorb sufficient amount of NO for its reduction with ammonia to  $\text{N}_2$  and  $\text{H}_2\text{O}$ . Secondly, increased oxygen vacancies in the sulfated samples due to reduction of  $\text{Ce}^{4+}$  to  $\text{Ce}^{3+}$  could also help in oxygen migration from bulk and adsorption from the gaseous phase.

This redox cycle is believed to be the reason for increased activity by fast SCR reaction at low temperatures in Ce-added catalysts [38,39].

Oxygen peak fits for as-prepared and sulfated catalysts are presented in Fig. 12. The peaks were deconvoluted into two:  $\text{O}_\alpha$  and  $\text{O}_\beta$ , as mentioned elsewhere [25]. After being sulfated, the amount of chemisorbed oxygen was increased which can be released during oxidation cycle. Since it could be more easily available to the surface than from the bulk, it could speed up the oxidation step in complete redox reaction. Fig. 13 presents the XPS peak fits for sulfur in the sulfated samples. All the sulfated catalysts exhibited  $\text{S}_{2p}$  peak in the range of 168.6–169.3 eV binding energy, which is characteristic for  $\text{S}^{6+}$  oxidation state in sulfate form [40,41]. This confirms the formation of sulfate species onto the sulfated catalysts. Again the amount of sulfur detected (Table 2), increased with increasing sulfation temperature, which proves higher amounts of the surface sulfate species formed.

Based on our characterization and activity results at low temperature ( $225^\circ\text{C}$ ), catalytic performance of the sulfated samples can be summarized as shown in Fig. 14. Excess ammonia adsorption onto low-temperature sulfated catalysts (Fig. S1a) can inhibit direct contact of gaseous NO with the activated  $\text{NH}_3$  and/or blocking of the active redox species. However its activity might be resulted from the reaction between adsorbed (Fig. S2) or gaseous NO and activated  $\text{NH}_3$ , as it showed highest NO desorption as compared to other sulfated samples. Moreover, since all  $\text{CeO}_2$  could not be sulfated at low temperature by sulfation pretreatment, NO reduction could also occur by the reaction between gaseous NO and  $\text{NH}_3$  activated by  $\text{CeO}_2$  and/or  $\text{V}_2\text{O}_5$  species. In case of high-temperature sulfated sample, sufficiently high amount of  $\text{NH}_3$  and NO adsorption along with more reducible species resulted in highest achievable activity among fresh and other sulfated catalysts.



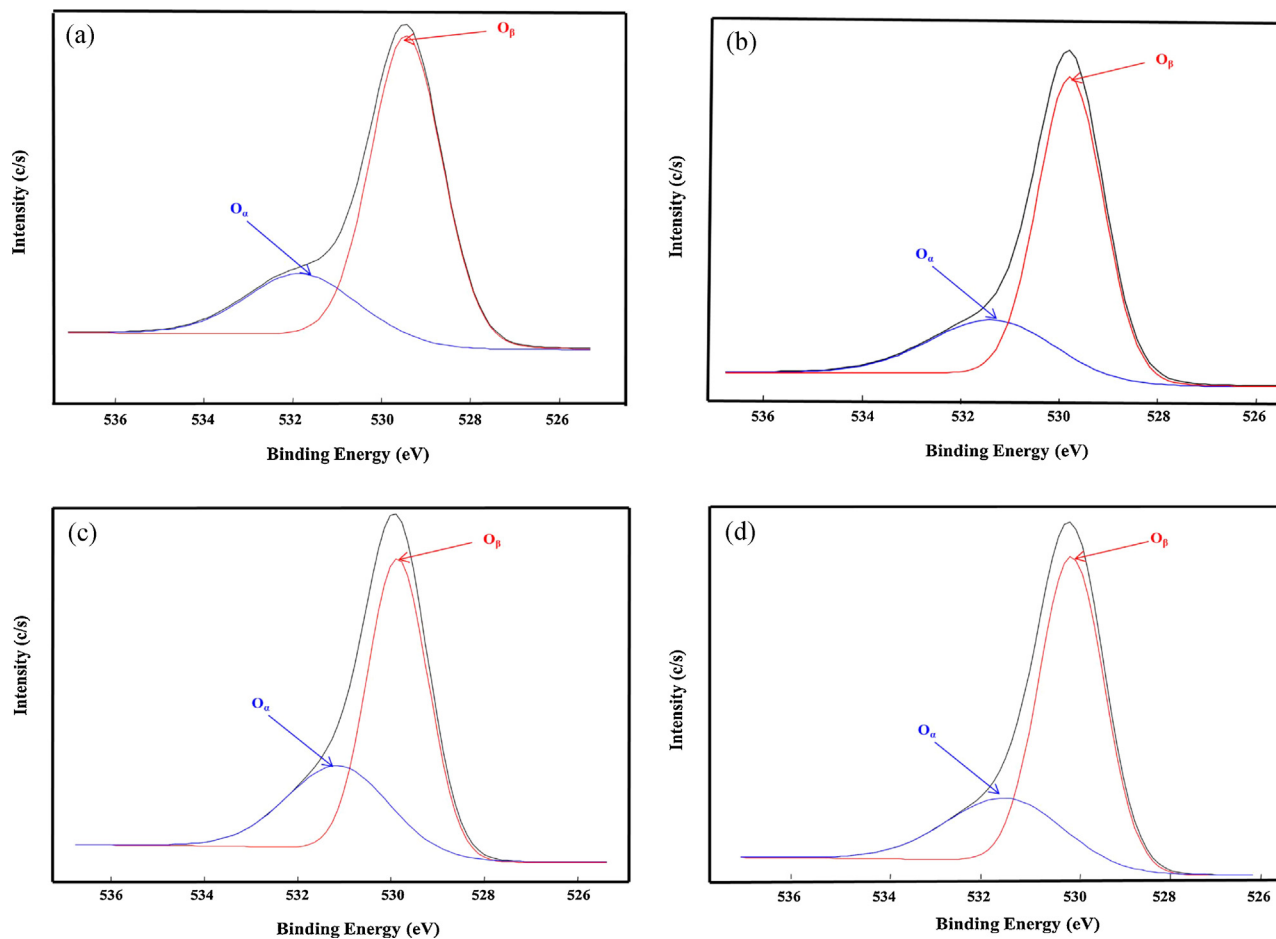


**Fig. 12.** XPS spectra of O 1s for the catalysts, as-prepared and sulfated at different temperatures: (a) as-prep., (b) S300, (c) S400, and (d) S500.

**Table 2**  
Elemental compositions (weight %) of cerium (Ce), oxygen (O) and sulfur (S) for fresh and sulfated catalysts.

Samples	Ce				O			S
	Ce <sup>+4</sup>	Ce <sup>+3</sup>	Ce <sub>total</sub>	O <sub>α</sub>	O <sub>β</sub>	O <sub>total</sub>	Surface (XPS)	Bulk (EDS)
As-prep.	47.1	52.9	0.72	24.7	75.3	76.3	–	–
S300	53.8	46.2	0.26	26.1	73.9	75.8	0.39	0.81
S400	39.9	60.1	0.34	26.9	73.1	67.6	0.76	0.93
S500	34.9	65.1	0.28	27.8	72.2	76.0	1.24	1.12

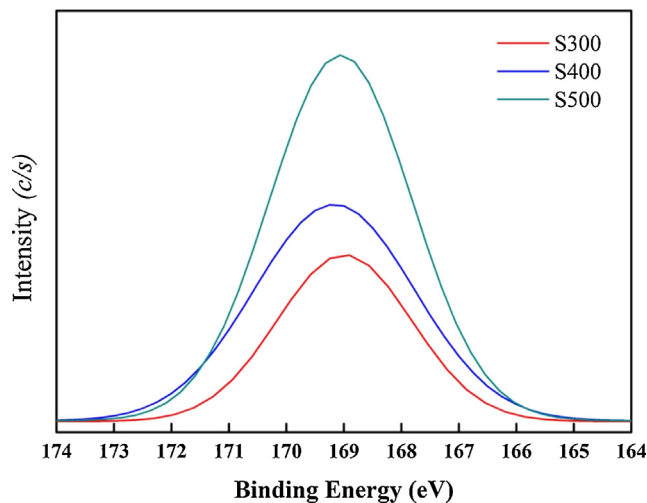


**Fig. 13.** XPS spectra of S 2p for the catalysts sulfated at different temperatures.

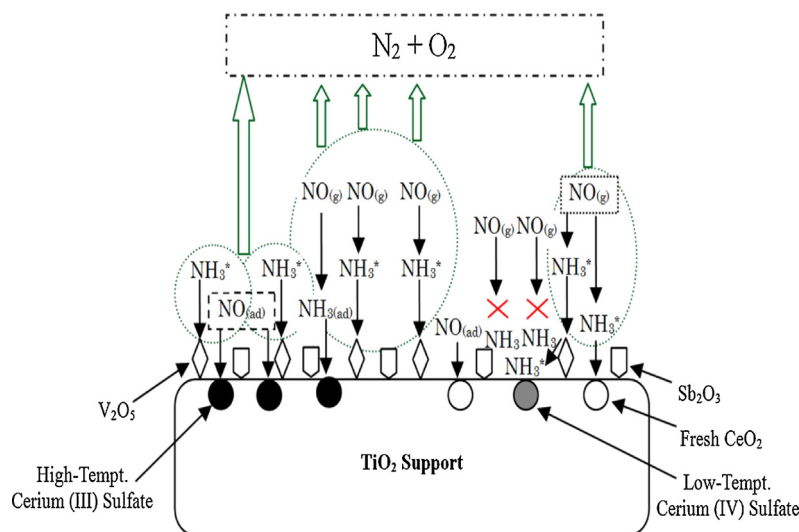


Fig. 14. Plausible reaction mechanism for sulfated catalysts at lower temperature ( $\approx 225^\circ\text{C}$ ).

#### 4. Conclusions

10%  $\text{CeO}_2$ -added,  $\text{Sb}/\text{V}_2\text{O}_5/\text{TiO}_2$  catalyst was pretreated with  $\text{SO}_2$  under oxidizing conditions at 300, 400 and  $500^\circ\text{C}$ , each for 2 h. The increase in surface area after sulfation could be due to amorphous nature of the sulfate species formed. No ceria peak was observed for the sulfated catalysts possibly due to poor  $\text{CeO}_2$  crystallinity after sulfation.  $\text{NH}_3$  adsorption was increased with increasing sulfation temperature, whereas  $\text{NO}$  adsorption tendency decreased due to increased acidity of the sulfated catalysts. The difference in  $\text{NH}_3$  and  $\text{NO}$  adsorption patterns suggested difference in nature of the sulfate species formed, which became clear from their mass spectra,  $\text{H}_2$ -TPR and XPS studies. S500 catalyst showed highest amount of available reducible species. XPS studies could detect increased  $\text{Ce}^{3+}$  species on the S500 catalyst, in contrast to the S300 sample with higher amount of  $\text{Ce}^{4+}$  species. Therefore, the high-temperature ( $500^\circ\text{C}$ ) sulfate species could be referred as  $\text{Ce}(\text{III})$  sulfate and those formed at low temperature ( $300^\circ\text{C}$ ) as  $\text{Ce}(\text{IV})$  sulfate. The activity results proved that the cerium(III) sulfate species formed at  $500^\circ\text{C}$  were more active, as compared to those formed at lower temperatures. Specifically, cerium(IV) sulfates formed at  $300^\circ\text{C}$  were found to be unfavorable for  $\text{NH}_3$ -SCR of  $\text{NO}_x$  for prolonged time periods at low temperatures, resulting in poisoning and deactivation of the catalyst.

#### Acknowledgements

This work was financially supported by 'Future Core Technology' program from KIST. The grant from 'Fundamental R&D Program for the Core Technology of Materials', funded by the Ministry of Knowledge Economy, Republic of Korea is also highly acknowledged.

#### Appendix A. Supplementary data

Supplementary data associated with this article can be found, in the online version, at <http://dx.doi.org/10.1016/j.apcatb.2014.01.017>.

#### References

- [1] P. Forzatti, Appl. Catal. A 222 (2001) 221–236.
- [2] P.S. Metkar, M.P. Harold, V. Balakotaiah, Appl. Catal. B 111–112 (2012) 67–80.
- [3] S. Roy, M.S. Hedge, G. Madras, Appl. Energy 86 (2009) 2283–2297.
- [4] G. Busca, L. Lietti, G. Ramis, F. Berti, Appl. Catal. B 18 (1998) 1–36.
- [5] M.D. Amiridis, R.V. Duevel, I.E. Wachs, Appl. Catal. B 20 (1999) 111–122.
- [6] S.T. Choo, S.D. Yim, I.S. Nam, S.W. Ham, J.B. Lee, Appl. Catal. B 44 (2003) 237–252.
- [7] C. Orsenigo, L. Lietti, E. Tronconi, P. Forzatti, F. Bregani, Ind. Eng. Chem. Res. 37 (1998) 2350–2359.
- [8] J.P. Dunn, J. Jehng, D.S. Kim, L.E. Briand, H.G. Stenger, I.E. Wachs, J. Phys. Chem. B 102 (1998) 6212–6218.
- [9] X. Guo, C. Bartholomew, W. Hecker, L.L. Baxter, Appl. Catal. B 92 (2009) 30–40.
- [10] A. Shi, X. Wang, T. Yu, M. Shen, Appl. Catal. B 106 (2011) 359–369.
- [11] M.D. Amiridis, I.E. Wachs, G. Deo, J.M. Jehng, D.S. Kim, J. Catal. 161 (1996) 247–253.
- [12] J.P. Chen, R.T. Yang, J. Catal. 125 (1990) 411–420.
- [13] F. Liu, K. Asakura, H. He, W. Shan, X. Shi, C. Zhang, Appl. Catal. B 103 (2011) 369–377.
- [14] N.Y. Topsoe, J.A. Dumesic, H. Topsoe, J. Catal. 151 (1995) 241–252.
- [15] R. Khodayari, C.U.I. Odenbrand, Appl. Catal. B 33 (2001) 277–291.
- [16] X. Du, X. Gao, L. Cui, Y. Fu, Z. Luo, K. Cen, Fuel 92 (2012) 49–55.
- [17] B. Thirupathi, P.G. Smirniotis, Appl. Catal. B 110 (2011) 195–206.
- [18] R. Jin, Y. Liu, Z. Wu, H. Wang, T. Gu, Chemosphere 78 (2010) 1160–1166.
- [19] X. Gao, Y. Jiang, Y. Zhong, Z. Luo, K. Cen, J. Hazard. Mater. 174 (2010) 734–739.
- [20] M. Luo, J. Chen, L. Chen, J. Lu, Z. Feng, C. Li, Chem. Mater. 13 (2001) 197–202.
- [21] L. Chen, J. Li, M. Ge, R. Zhu, Catal. Today 153 (2010) 77–83.
- [22] L. Chen, J. Li, M. Ge, L. Ma, H. Chang, Chin. J. Catal. 32 (2011) 836–841.
- [23] H. Chang, X. Chen, J. Li, L. Ma, C. Wang, C. Liu, J.W. Schwank, J. Hao, Environ. Sci. Technol. 47 (2013) 5294–5301.
- [24] T. Gu, Y. Liu, X. Weng, H. Wang, Z. Wu, Catal. Commun. 12 (2010) 310–313.
- [25] K.J. Lee, A.K. Pullur, M.S. Maqbool, K.N. Rao, K.H. Song, H.P. Ha, Appl. Catal. B 142–143 (2013) 705–717.
- [26] K.J. Lee, M.S. Maqbool, A.K. Pullur, Y.E. Jeong, K.H. Song, H.P. Ha, Res. Chem. Intermediat. (2013).
- [27] S. Yang, Y. Guo, H. Chang, L. Ma, Y. Peng, Z. Qu, N. Yan, C. Wang, J. Li, Appl. Catal. B 136–137 (2013) 19–28.
- [28] H.P. Ha, M.P. Reddy, A.K. Pullur, K.J. Lee, S.H. Jung, Appl. Catal. B 78 (2008) 301–308.
- [29] J.W. Choung, I.S. Nam, S.W. Ham, Catal. Today 111 (2006) 242–247.
- [30] G. Xie, Z. Liu, Z. Zhu, Q. Liu, J. Ge, Z. Huang, J. Catal. 224 (2004) 42–49.
- [31] X. Gao, X. Du, L. Cui, Y. Fu, Z. Luo, K. Cen, Catal. Commun. 12 (2010) 255–258.
- [32] I. Nova, C. Ciardelli, E. Tronconi, AIChE J. 52 (2006) 3222–3233.
- [33] C. Gannoun, R. Delaigle, D.P. Debecker, P. Eloy, A. Ghorbel, E.M. Gaigneaux, Appl. Catal. A 447–448 (2012) 1–6.
- [34] L. Baraket, A. Ghorbel, P. Grange, Appl. Catal. B 72 (2007) 37–43.
- [35] H. Tagawa, Thermochim. Acta 80 (1984) 23–33.
- [36] J.A. Poston Jr., R.V. Siriwardane, E.P. Fisher, A.L. Miltz, Appl. Surf. Sci. 214 (2003) 83–102.
- [37] K.J. Lee, M.S. Maqbool, A.K. Pullur, K.H. Song, H.P. Ha, Catal. Lett. 143 (2013) 988–995.
- [38] B. Murugan, A.V. Ramaswamy, J. Am. Chem. Soc. 129 (2007) 3062–3063.
- [39] C.T. Campbell, C.H.F. Peden, Science 309 (2005) 713–714.
- [40] G. Xie, Z. Liu, Z. Zhu, Q. Liu, J. Ma, Appl. Catal. B 45 (2003) 213–221.
- [41] C.H. Wang, C.N. Lee, H.S. Weng, Ind. Eng. Chem. Res. 37 (1998) 1774–1780.